Journal of Integrative Agriculture 2026, 25(9): 3537–3547

Available online at ScienceDirect

Journal of Integrative Agriculture

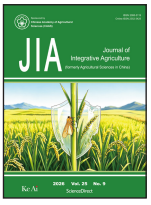

RESEARCH ARTICLE

TaRLK-1B: A novel wheat gene conferring resistance to leaf rust revealed by a genome-wide association study

Shujuan Liu[1, 2*], Li Zhao[1, 2*], Chenyang Hao[2*], Yuxue Pan[2], Mengjiao Guo[2], Yilin Huang[2], Haixia Liu[2], Jian Hou[2], Zaifeng Li[3#], Tian Li[2#], Xinhong Chen[1#], Xueyong Zhang[2#]

[1] *Shaanxi Key Laboratory of Plant Genetic Engineering Breeding/College of Agronomy, Northwest A&F University, Yangling 712100, China*
[2] *State Key Laboratory of Crop Gene Resources and Breeding/Institute of Crop Sciences, Chinese Academy of Agricultural Sciences, Beijing 100081, China*
[3] *College of Plant Protection, Hebei Agricultural University, Baoding 071001, China*

Highlights

- The wheat leaf rust resistance gene *TaRLK-1B* was identified through genome-wide association study in the advanced backcross-nested association mapping plus inter-crossed population.
- *TaRLK-1B* positively regulates resistance to leaf rust in wheat.
- Pyramiding of minor-effect QTLs significantly enhances resistance to leaf rust in wheat.

Abstract

Leaf rust is a highly destructive foliar disease in wheat which causes major constraints in wheat production worldwide. In this study, we conducted a comprehensive assessment of adult plant resistance to leaf rust in 590 accessions from the advanced backcross-nested association mapping plus inter-crossed (AB-NAMIC) population. We used 660K genotype data to perform a genome-wide association study (GWAS), which identified significant quantitative trait loci (QTLs) on chromosomes 1B, 2A, 2B, and 7D, and then focused on the candidate gene *TaRLK-1B* on chromosome 1B. A cleaved amplified polymorphic sequence (CAPS) marker developed based on *TaRLK-1B* haplotypes could effectively differentiate between resistant and susceptible varieties. This gene encodes a membrane-localized leucine-rich repeat receptor-like kinase (LRR-RLK) that is upregulated in response to the fungal infection that causes leaf rust. Targeted knockout of *TaRLK-1B* in wheat led to reduced resistance to leaf rust, underscoring its essential role as a positive regulator of the defense against this disease. We propose that TaRLK-1B interacts with the receptor-like cytoplasmic kinase TaRLCK1B, potentially facilitating immune signal transduction. Our findings also demonstrate that pyramiding minor effect QTLs significantly increases resistance to leaf rust. This study provides novel insights into rust resistance genes and valuable QTL information, which can improve marker-assisted wheat breeding efforts.

Keywords: GWAS, LRR-RLK, resistance gene, leaf rust, wheat

1. Introduction

Wheat leaf rust, also known as brown rust, is caused by the fungal pathogen *Puccinia triticina* (*Pt*) and a major constraint on the global wheat grain yield (Prasad *et al*. 2020). The high adaptability and widespread presence of leaf rust in wheat-growing regions result in leaf damage that impairs photosynthesis, ultimately reducing both yield and wheat quality (Huerta-Espino *et al*. 2011). Leaf rust causes an estimated production loss of approximately 25 million tons annually (Kolmer 2013; Savary *et al.* 2019). To date, a total of 85 genes conferring resistance to wheat leaf rust have been formally identified in both wheat and its wild relatives (Sharma *et al.* 2024). However, the complex and extensive wheat genome has posed challenges for gene cloning, and

Received 21 October 2024; Received in revised form 20 November 2024; Accepted 13 January 2025; Available online 18 February 2025
[#]Correspondence Xueyong Zhang, E-mail: zhangxueyong@caas.cn; Xinhong Chen, E-mail: cxh2089@126.com; Tian Li, E-mail: litian@caas.cn; Zaifeng Li, E-mail: lzf7551@aliyun.com
[*] These authors contributed equally to this study.

doi: 10.1016/j.jia.2025.02.028

only 12 genes have been successfully cloned to date: *Lr1*, *Lr9*, *Lr10*, *Lr13*, *Lr14a*, *Lr21*, *Lr22a*, *Lr34*, *Lr42*, *Lr47*, *Lr67*, and *Lr85* (Feuillet *et al.* 2003; Huang *et al.* 2003; Cloutier *et al.* 2007; Krattinger *et al.* 2009; Moore *et al.* 2015; Thind *et al.* 2017; Kolodziej *et al.* 2021; Yan *et al.* 2021; Lin *et al.* 2022; Li *et al.* 2023; Wang *et al.* 2023; Sharma *et al.* 2024). The number of cloned wheat genes related to resistance to leaf rust is limited, and individual resistance genes may carry undesirable agronomic traits, making wheat vulnerable to the evolving strains of this pathogen (Dracatos *et al.* 2023). Although chemical pesticides offer a direct method of rust control, their excessive use poses risks of environmental contamination and food safety hazards (Figueroa *et al.* 2018). Therefore, deploying disease resistance genes and cultivating resistant varieties have emerged as the most effective strategies for managing leaf rust.

A significant reduction in sequencing costs has facilitated the widespread adoption of high-density DNA markers which enable more effective detection of minor-effect QTLs (Yao *et al.* 2020; Hao *et al*. 2024). Genome-wide association studies (GWASs), which leverage whole-genome resequencing, have become pivotal in wheat disease resistance research (Demirjian *et al.* 2023). Thus far, 296 QTLs conferring resistance to leaf rust have been identified in the wheat genome (Tong *et al.* 2024). For example, the 90K Illumina iSelect SNP array was used to genotype 268 wheat lines, and a GWAS identified 22 seedling-stage QTLs and 22 adult-stage QTLs associated with resistance to leaf rust (Zhang *et al.* 2021). A comprehensive phenotypic evaluation of 365 bread wheat varieties was conducted using four *Pt* strains, followed by a GWAS with 302,524 high-quality single-nucleotide polymorphisms (SNPs), which revealed 27 significant marker-trait associations (MTAs) associated with resistance to leaf rust (Kaur *et al.* 2023). These findings pave the way for the use of marker-assisted selection to develop leaf rust resistance cultivars in wheat.

Leucine-rich-repeat receptor-like kinases (LRR-RLKs) are one of the largest and most conserved subfamilies of RLKs in plants, and they play crucial roles in initiating plant defense responses (Shiu and Bleecker 2001; Smakowska-Luzan *et al.* 2018). *TaRLK1* and *TaRLK2* are among the earliest characterized *LRR-RLKs* in wheat, and the overexpression of these genes increases wheat resistance to powdery mildew (Chen *et al.* 2016). TaXa21, an LRR-RLK with high homology to the rice bacterial blight resistance protein Xa21, interacts with TaWRKY76 and TaWRKY62 to positively regulate high-temperature resistance to stripe rust in wheat seedlings (Wang *et al.* 2019). Furthermore, *AcRLK2P-1* derived from *Agropyron cristatum* confers resistance to multiple leaf rust races (Xu *et al.* 2024; Ji *et al*. 2025). This finding highlights the complex and layered nature of plant immune signaling, in which RLKs are essential for orchestrating effective defense strategies.

To date, the cloning and functional validation of wheat genes conferring resistance to leaf rust identified *via* GWASs have been rarely reported. In this study, the phenotypes of plants with adult-stage leaf rust resistance in the advanced backcross-nested association mapping plus inter-crossed (AB-NAMIC) population were determined, and four QTLs associated with resistance were identified through GWAS. One of candidate genes that positively regulate resistance to leaf rust, *TaRLK-1B* located on chromosome 1B, was identified and validated. A gene-specific marker for *TaRLK-1B* was developed which provides an available marker to combine with other QTLs to enhance leaf rust resistance in wheat. These findings provide valuable insights for developing leaf rust-resistant wheat varieties and offer potential applications in molecular marker-assisted breeding programs.

2. Materials and methods

2.1. Plant materials

The AB-NAMIC population was constructed by crossing three elite modern Chinese cultivars (Zhoumai 18, Zhengmai 366, and Handan 6172) with 20 accessions from the mini-core germplasm as recurrent founders (Jiao *et al.* 2023). A subset of 590 lines from this population was genotyped using a 660K SNP array (Affymetrix Axiom Wheat660). Experiments involving wheat and *Nicotiana benthamiana* plants were conducted under controlled environmental conditions in a greenhouse. The greenhouse temperature was maintained at 22°C/20°C (day/night) for wheat and 25°C/22°C (day/night) for *N. benthamiana*. Plants were subjected to an extended photoperiod of 16 hours of light followed by 8 hours of darkness.

2.2. Phenotypic evaluation of leaf rust resistance

The AB-NAMIC population was cultivated at the Xinxiang Experimental Station, Chinese Academy of Agricultural Sciences (CAAS) (113.5°E, 35.2°N). Each accession was planted in a 4-m, four-row plot with rows spaced 25 cm apart and containing 40 seeds per row. Susceptible wheat variety Mingxian 169 (MX169) was used as a control and inoculum spreader to ensure consistent disease development across the field. Severe outbreaks of natural leaf rust disease occurred in the field in 2016, 2017, and 2022. Phenotypic evaluation was based on infection type and scored on a scale from 0 to 4, representing a range from immunity to severe infection (Pang *et al.* 2021; Jiao *et al.* 2023). Disease assessments were conducted at least twice when the susceptible control showed significant disease symptoms to ensure the reliability of the phenotypic data. The final infection type recorded was used for phenotype determination.

Seedling-stage inoculation with the leaf rust race and phenotypic evaluation followed established protocols (Huai *et al.* 2022; Liu *et al.* 2024). The highly virulent *Pt* race THT was isolated from infected leaves of MX169. Seedling-stage inoculation was performed using a spray method on wild-type (WT) and *TaRLK-1B* KO lines at the two-leaf stage. Two weeks after inoculation, the percentage of leaf area covered by pustules on the inoculated leaves was quantified on a scale from 0 to 100% (modified Cobb scale), and photographs were taken to document the phenotypic characteristics of the diseased leaves. Agronomic traits of the T_3 generation KO and WT plants were evaluated at the CAAS experimental field in Shunyi, Beijing (116.65°E, 40.13°N).

2.3. Genome-wide association study (GWAS)

A mixed linear model (MLM) implemented in the lme4 package of R (version 3.2.2) was used to estimate best linear unbiased prediction (BLUP) values for each line and calculate the broad-sense heritability of the AB-NAMIC population (Jiao *et al.* 2023). The GWAS analysis for leaf rust resistance, incorporating three years of field phenotypic data and corresponding BLUP values from the AB-NAMIC population, was conducted using EMMAX software (Kang *et al.* 2010). The kinship matrix calculated by EMMAX was included as a random effect to adjust the association results, with a significance threshold of $P<1.0\times10^{-5}$ to increase GWAS precision (Kang *et al.* 2010). The Q matrix, used to correct for population structure, was generated using the first three principal components calculated with GCTA software (Yang *et al.* 2011). Manhattan and quantile-quantile (QQ) plots were generated with the R package CMplot (available at https://github.com/YinLiLin/R-CMplot). Pairwise linkage disequilibrium (LD) among the SNPs flanking each QTL was graphically represented using the R package LDheatmap (Shin *et al.* 2006). In addition, the BLUP values combined with the MLM in the GAPIT package were used to analyze the phenotypic variance explained (PVE) by significant SNPs ($-\log_{10}(P)\geq5$) (Zhang *et al.* 2010). Correlation coefficients between phenotypic traits across different environments and normal distributions were plotted using the corrplot and ggplot2 packages in R.

2.4. Candidate gene prediction and functional marker development

Regions flanking significant SNPs by 1 Mb were designated candidate QTL intervals. Annotated genes within these QTL regions were extracted from the wheat Chinese Spring reference genome version 1.1. The gene expression database from the Wheatomics 1.0 website (http://202.194.139.32/) was used to analyze the tissue-specific expression patterns of the candidate genes.

A cleaved amplified polymorphic sequence (CAPS) marker was developed based on a SNP (T/G at 2,812 bp) that can distinguish between resistant and susceptible haplotypes using the restriction endonuclease NheI-HF (New England Biolabs, Beijing, China), and the AB-NAMIC population was employed for validation. Subsequently a comprehensive significance test was performed to correlate genotypes with the corresponding phenotypes (BLUP values).

2.5. Generation of *TaRLK-1B* KO lines

For the *TaRLK-1B* KO construct, two single-guide RNAs (sgRNAs) were designed to target the *TaRLK-1B* homologues. These sgRNA sequences (CCATTCCTCCTAG CCTAGGAAAC and CCAACTCTCGGGCCAGATACCTC) were subsequently cloned and inserted into the pBUE411 vector for CRISPR/Cas9-mediated genome editing (Liu *et al.* 2023). The constructs were subsequently introduced into *Agrobacterium tumefaciens* strain EHA105 and transformed into immature embryos of the wheat variety Jimai 38, which carries the Hap-R allele of *TaRLK-1B*, using the *Agrobacterium*-mediated transformation method (Li *et al.* 2021). Phenotypic evaluation was carried out on the T_3 generation of the *TaRLK-1B* KO lines.

2.6. Subcellular localization

The full-length coding sequence (CDS) of *TaRLK-1B* was cloned and inserted into the pCAMBIA1300-GFP vector. The resulting construct was transformed into *A. tumefaciens* strain GV3101 cells, which were then used to infiltrate *N. benthamiana* leaves. GFP fluorescence was observed at 60 h after infiltration using an LSM880 laser-scanning confocal microscope (Carl Zeiss, Germany) with excitation at 488 nm.

2.7. Characterization of TaRLK-1B

Protein domain architecture was predicted using the SMART database (https://smart.embl-heidelberg.de/). Transmembrane topology prediction was performed using the DeepTMHMM online tool (https://dtu.biolib.com/DeepTMHMM). Multiple sequence alignment of the 11 LRR domains was performed with DNAMAN software. A phylogenetic tree was constructed using the neighbor-joining (NJ) method in MEGA7 software, with a bootstrap value of 1,000.

2.8. Reverse transcription quantitative PCR (RT-qPCR) analysis

For the RT-qPCR analysis, the wheat cultivar Fielder was inoculated with the *Pt* race THT, and samples were collected for RNA extraction at 0–120 hours post-inoculation (hpi). Total RNA was extracted using the RNAiso Plus reagent according to the manufacturer's protocol (TaKaRa, Japan), and 2 μg of RNA was reverse transcribed using the FastQuant RT Kit (Tiangen, Beijing, China). RT-qPCR assays were performed on a LightCycler 96 Real-Time PCR System (Roche Applied Science, Mannheim, Germany) with SYBR Premix *Ex Taq* (TaKaRa). The relative expression fold-changes of the genes were calculated using the comparative cycle threshold (CT) method, with the *TaActin* gene serving as the internal reference (Appendix A). All assays were conducted in triplicate and independently repeated three times (Jian *et al.* 2022).

2.9. Luciferase complementation imaging (LCI) assays

The full-length CDSs of *TaRLK-1B* and *TaRLCK1B* (*TraesCS1B02G038800.1*) were fused to the N- and C-termini of the luciferase reporter gene (*LUC*), respectively. The resulting nLUC and cLUC constructs were transformed into *A. tumefaciens* strain GV3101 cells, which were then co-infiltrated into *N. benthamiana* leaves. LUC activity was imaged at 60 h after infiltration using the Night SHADE LB 985 Plant Imaging System (Berthold Technologies, Bad Wildbad, Germany).

3. Results

3.1. GWAS for leaf rust resistance

A phenotypic evaluation of leaf rust resistance was conducted on 590 adult-stage accessions of the AB-NAMIC population, with the average disease infection type ranging from level 0 to level 4 (Fig. 1-A). A frequency distribution analysis of the disease infection type data

collected over three years (2016, 2017, and 2022) under conditions of severe natural disease incidence revealed an approximately normal distribution, suggesting polygenic control with minor-effect genes (Fig. 1-B). Correlation coefficients among the four environments were highly significant ranging from 0.14 to 0.69 (Appendix B). The phenotypic variation rate ranged from 34.05 to 53.15%, with a broad-sense heritability of 0.54, indicating extensive and representative phenotypic variation among the population accessions (Appendix C). The AB-NAMIC population was genotyped using the 660K SNP array. Comprehensive GWAS analysis using an MLM identified a total of 99 SNPs significantly associated with wheat leaf rust resistance that surpassed the threshold of 1.0×10^{-5} (Fig. 1-C and D). These significant SNPs were distributed across multiple chromosomes, including one SNP on chromosome 1A, 79 SNPs on chromosome 1B, 12 SNPs on chromosome 2A, three SNPs on chromosome 2B, and four SNPs on chromosome 7D. Collectively, these SNPs explained 0.46 to 9.57% of the total phenotypic variation (Fig. 1-C; Appendix D).

3.2. Prediction of candidate genes associated with leaf rust resistance

The majority of the 99 significant SNPs identified were located on the long arm of chromosome 1B, collectively contributing 5.34 to 7.95% of the phenotypic variation (Appendix D). A QTL on chromosome 1B harbored the largest number of significant SNPs and exhibited the highest $-\log_{10}(P)$ value, approaching 8. This QTL was therefore selected for further investigation (Fig. 2-A). A 1 Mb genomic interval (666,886,444–668,886,444 bp) flanking the most significant SNP on chromosome 1B was identified as the candidate QTL interval for disease resistance. A total of 41 genes were annotated in this region, seven of which were identified as candidate genes related to disease resistance. These candidate genes included four genes encoding nucleotide-binding leucine-rich repeat receptors (NLRs) (*TraesCS1B02G447000*, *TraesCS1B02G447200*, *TraesCS1B02G447300*, and *TraesCS1B02G447400*), one gene encoding a peroxisomal membrane protein (*TraesCS1B02G447500*), one gene encoding an LRR-RLK (*TraesCS1B02G448700*), and one gene encoding a kinase (*TraesCS1B02G450700*).

Three of these genes encoding one NLR (*TraesCS1B02G447400*), the peroxisomal membrane protein (*TraesCS1B02G447500*), and the kinase (*TraesCS1B02G450700*), exhibited no SNP variations in either the coding or promoter regions, thereby refining the scope of the candidate genes (Appendix E).

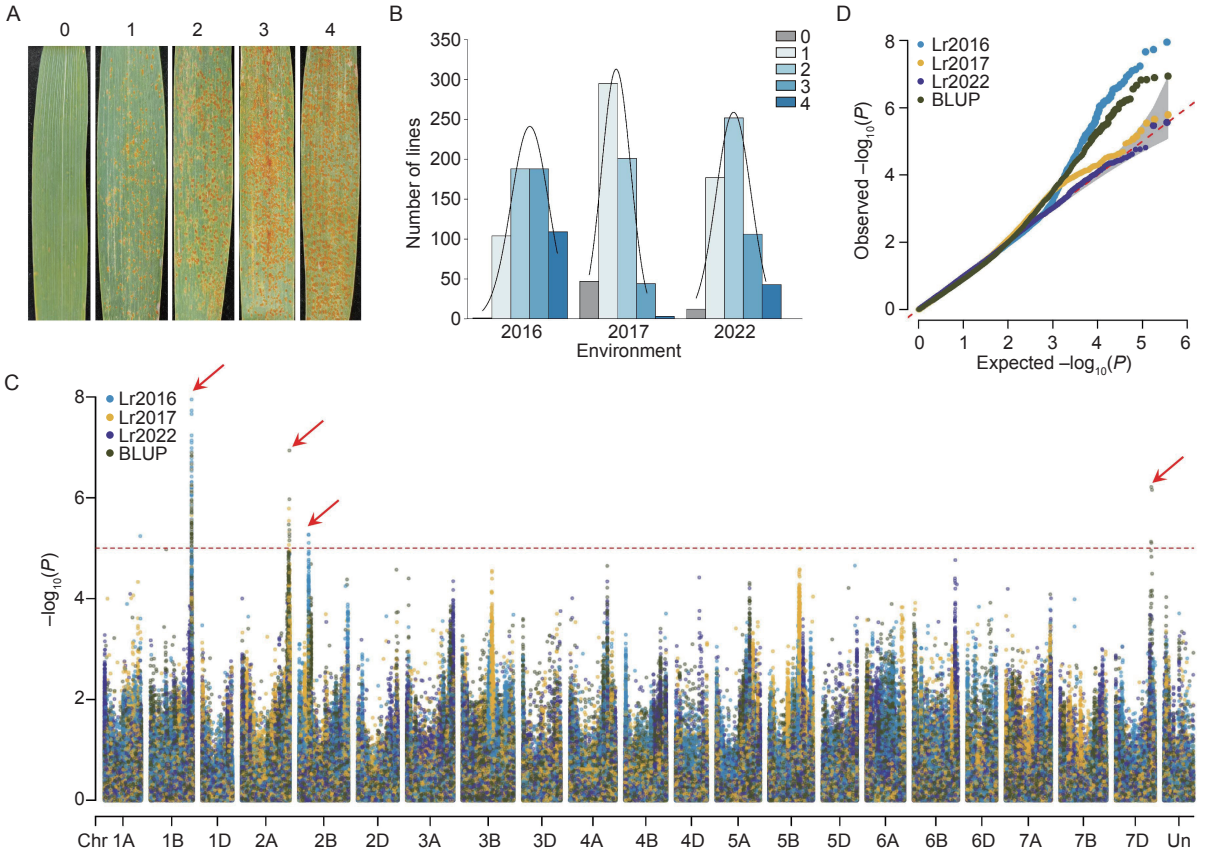

Fig. 1 Genome-wide association study (GWAS) on adult-stage responses to *Puccinia triticina* in the advanced backcross-nested association mapping plus inter-crossed (AB-NAMIC) panel. A, phenotypes corresponding to the classification of wheat adult-stage responses to *P. triticina*. Infection types were classified as 0–4. B, mean infection type (IT) frequency distributions for the AB-NAMIC panel grown at Xinxiang, Henan Province, China in different years. C, Manhattan plots for the GWAS of resistance to leaf rust in the AB-NAMIC panel. The red dotted line indicates the significance threshold set at $P=1.0\times10^{-5}$ and the red arrows represent significant QTLs that exceed the threshold. D, QQ plot for the GWAS population. Lr, leaf rust; BLUP, best linear unbiased prediction.

The remaining four candidate genes were subsequently subjected to a detailed tissue-specific expression pattern analysis. The results revealed that three other *NLR* genes were predominantly expressed in wheat roots, with minimal expression in stems and leaves, and they were not induced by *Pt* infection (Fig. 2-B; Appendix F). In contrast, the LRR-RLK-encoding gene (*TraesCS1B02G448700*) was highly expressed in stems, leaves, and spikes, with no expression in the roots, and harbored two non-synonymous mutations (Fig. 2-B; Appendix E). Consequently, this gene was considered the most likely candidate gene for leaf rust resistance on chromosome 1B, which we designated as *TaRLK-1B*.

3.3. Haplotype analysis and gene specific marker development for *TaRLK-1B*

To explore the genetic diversity of *TaRLK-1B* across different accessions, the *TaRLK-1B* alleles were sequenced from five accessions exhibiting extreme resistance to leaf rust and five displaying extreme susceptibility to leaf rust. Sequencing analysis revealed that the *TaRLK-1B* gene spans 3,564 bp, with a CDS of 3,219 bp that translates into a protein of 1,072 amino acids. Its gene structure consists of two exons and one intron. A comparative analysis between resistant and susceptible accessions revealed five SNPs, four of which caused non-synonymous mutations, resulting in two distinct haplotypes: the resistant haplotype (Hap-R) and the susceptible haplotype (Hap-S) (Fig. 3-A). The SNP at position 2,812 bp was leveraged to develop a CAPS marker for genotyping within the AB-NAMIC population. Hap-R was identified by the presence of undigested products after digestion with the NheI enzyme, whereas Hap-S was distinguished by the presence of digested products (Fig. 3-B). Furthermore, an association analysis linking phenotypic BLUP values with the identified haplotypes revealed that Hap-R accessions presented increased resistance to leaf rust compared with Hap-S accessions (Fig. 3-C). These findings validate the utility of the CAPS marker for distinguishing between resistant and susceptible haplotypes.

3.4. Characterization and expression analysis of *TaRLK* homoeologs in wheat

To determine the subcellular localization of TaRLK-1B, the full-length gene was fused to the N-terminus of GFP. Transient expression of the resulting fusion protein in *N. benthamiana* leaves revealed that TaRLK-1B is localized to the plasma membrane (Fig. 4-A). A bioinformatic analysis revealed several domains within TaRLK-1B, including a signal peptide domain, a tandem leucine-rich repeat domain flanked by cysteine-rich regions, 11 leucine-rich repeat domains, a transmembrane domain, and a serine/threonine protein kinase domain (Appendix G). A phylogenetic analysis placed TaRLK-1B closest to AtEFR, indicating its classification within the LRR–RLK family (Appendix H). The active kinase site of TaRLK-1B is similar to those of other proteins involved in pathogen recognition and the immune response, such as FLS2, EFR, and Xa21. This conservation classifies TaRLK-1B as a non-RD kinase within the XII family of LRR-RLKs (Appendix I). An analysis of the spatiotemporal expression pattern of TaRLK-1B revealed that *TaRLK* homoeologs are predominantly expressed in wheat leaves during early developmental stages, with constitutive expression in stems, leaves, and spikes

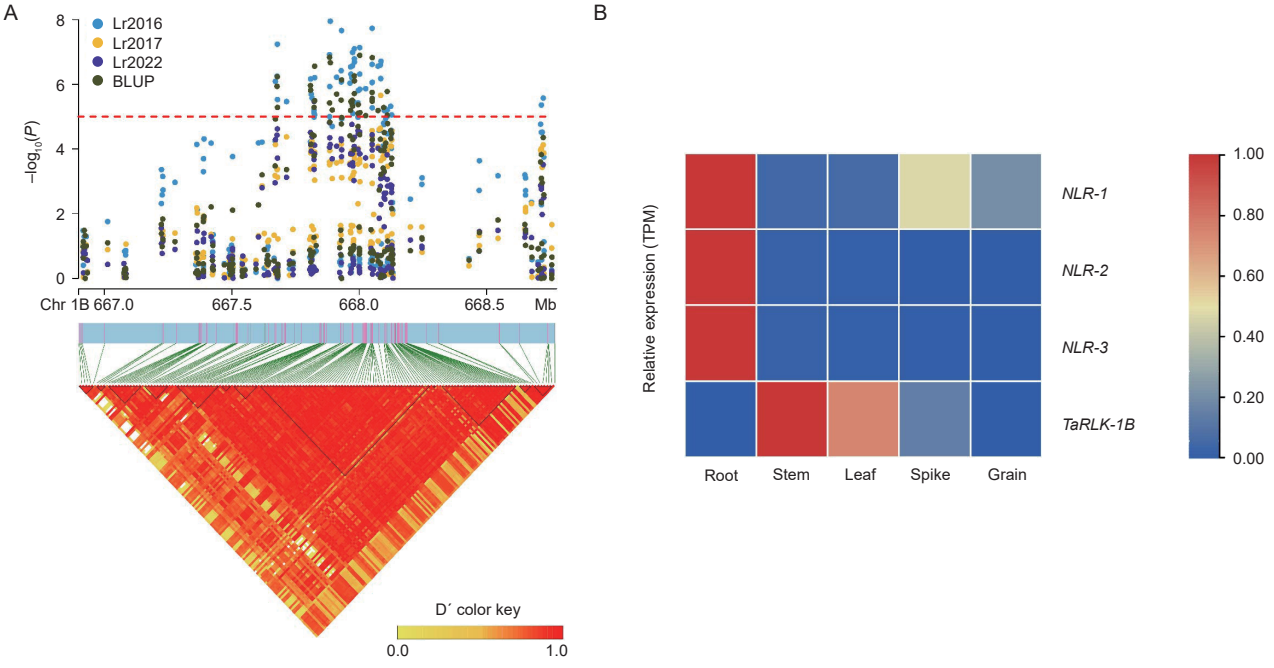

Fig. 2 Identification of candidate genes for resistance to leaf rust on chromosome 1B. A, local Manhattan plot (top) and linkage disequilibrium heatmap (bottom) for the region surrounding the peak single-nucleotide polymorphisms (SNP) on chromosome 1BL. Plots above the red line show genome-wide significance with a moderately stringent threshold (P=1.0×10^{-5}). B, expression heatmap of candidate genes within the block region in different tissues. Lr, leaf rust; BLUP, best linear unbiased prediction. TPM, transcripts per million.

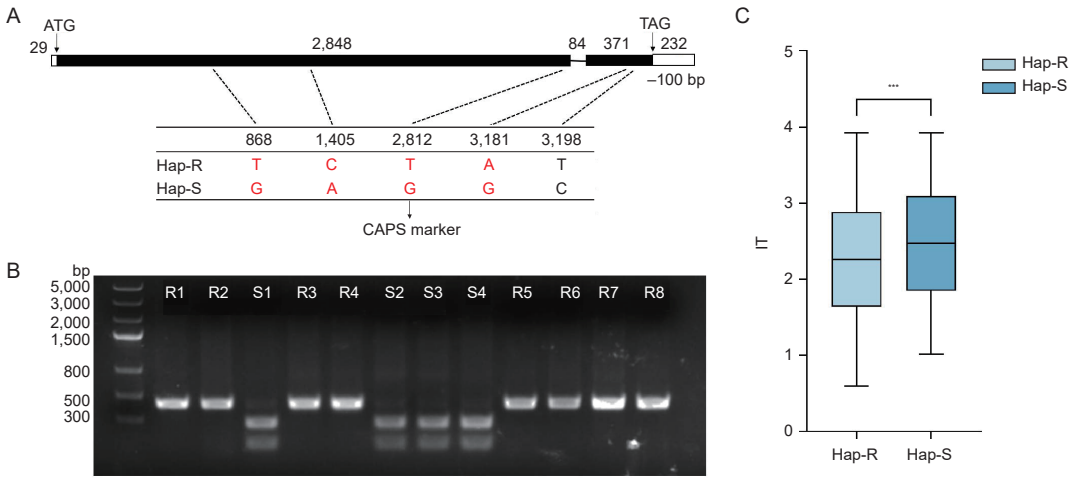

Fig. 3 *TaRLK-1B* was significantly associated with wheat leaf rust. A, gene structure and haplotype analyses of *TaRLK-1B*. Rectangles and lines represent exons and introns, respectively. Coding sequences are highlighted in black, and the UTRs are indicated with white rectangles. SNPs highlighted in red cause nonsynonymous mutations. Black arrows represent the SNPs marked by the developed CAPS marker. B, genotyping results of different accessions for the CAPS marker developed for *TaRLK-1B*. R, resistant haplotype; S, susceptible haplotype. C, boxplot of the haplotype-phenotype association analysis of *TaRLK-1B* based on the best linear unbiased prediction (BLUP) values. Box edges represent the 0.25 and 0.75 quantiles, with median values indicated by the middle lines. IT, infection type. ***, $P<0.001$ (Student's *t*-test).

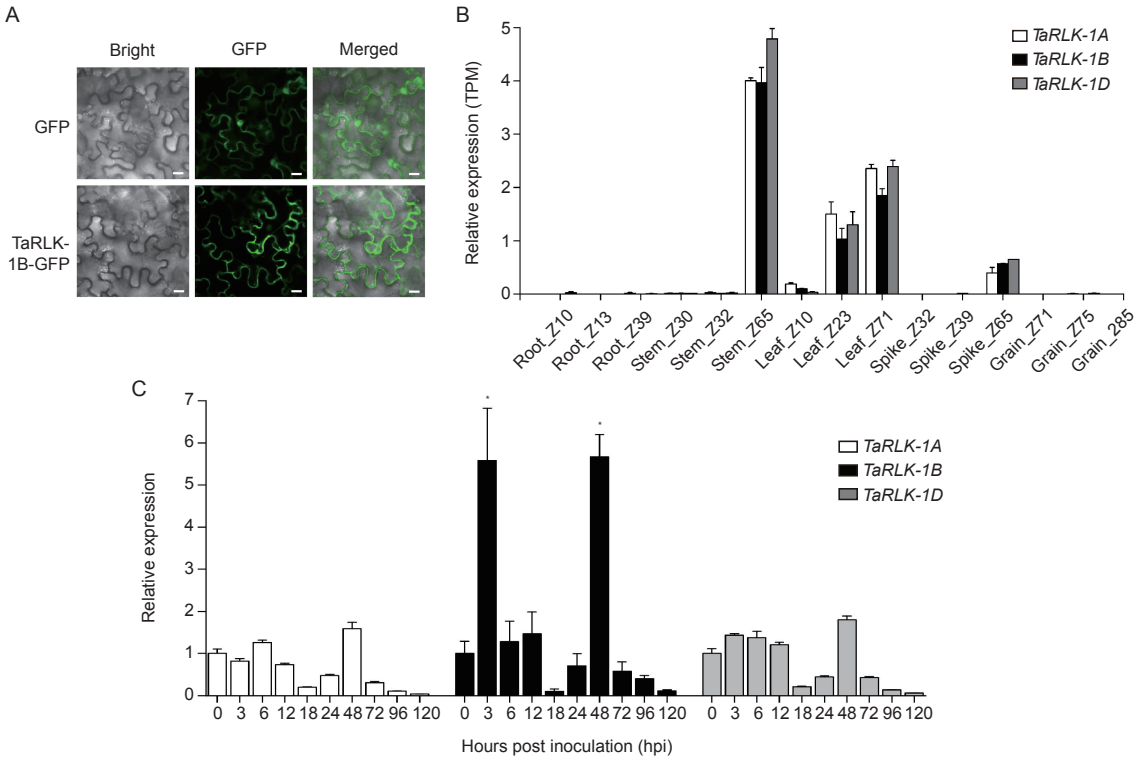

Fig. 4 Characterization of *TaRLK-1B*. A, subcellular localization of TaRLK-1B in tobacco leaves. The GFP and TaRLK-1B-GFP fusions were under the control of the CaMV 35S promoter. Scale bars, 20 μm. B, spatial and temporal expression patterns of the three *TaRLK* homoeologs. TPM, transcripts per million. C, relative expression levels of the three *TaRLK* homoeologs at different stages of *Pt* infection. *TaActin* was used for normalization. Data from three replicates are presented as the mean±SD (Student's *t*-test; *, $P<0.05$).

during later stages (Fig. 4-B). This expression pattern is consistent with the typical progression of leaf rust disease in wheat, which predominantly affects stems, leaves, and spikes in the later growth stages. Furthermore, *TaRLK-1B* was significantly induced in response to *Pt* infection, in contrast to the minimal responses observed for *TaRLK-1A* and *TaRLK-1D* (Fig. 4-C). Specifically, *TaRLK-1B* was significantly induced at the 3 hpi time point, highlighting its role in the early response to *Pt* infection.

3.5. *TaRLK-1B* positively regulates leaf rust resistance

To investigate the role of *TaRLK-1B* in the defense against leaf rust, knockout (KO) lines of the target gene were generated in the hexaploid wheat cultivar Jimai 38 using CRISPR/Cas9 technology. Sequencing confirmed successful gene editing of the three *TaRLK* homoeologs in the KO lines (Fig. 5-A), and three independent KO lines were selected for phenotypic evaluation. Fourteen days after inoculation with *Pt*, WT leaves showed no spore production, with only a few necrotic chlorotic spots. In contrast, the KO lines presented the significant presence of uredia, accompanied by extensive necrotic chlorotic areas on the leaf surface (Fig. 5-B and C). Notably, the key agronomic traits of the KO lines were not significantly different from those of the WT plants under field conditions (Appendix J).

In the context of plant immunity, RLKs perceive external signals through their extracellular domains and initiate downstream signaling pathways *via* their intracellular kinase domains (Couto and Zipfel 2016). These kinase domains phosphorylate various substrates, including RLKs, RLCKs, and MAPKs, thereby initiating signal transduction (Ngou *et al*. 2022). Given that *TaRLK-1B* encodes a membrane-localized receptor kinase, we hypothesized that *TaRLK-1B* potentially interacts with specific RLCKs in wheat to activate downstream signaling pathways. TaRLCK1B is a receptor-like cytoplasmic kinase that has been previously implicated in resistance to sharp eyespot in wheat (Wu *et al*. 2020). The physical interaction was confirmed with an LCI assay and the interaction between TaRLK-1B and TaRLCK1B was observed in tobacco, suggesting that TaRLK-1B conveys immune signals through TaRLCK1B (Appendix K). The loss of *TaRLK-1B* function reduced wheat resistance to *Pt*, indicating that TaRLK-1B acts as a positive regulator in the defense against leaf rust.

3.6. Analysis of QTL pyramiding effects

The impact of various combinations of QTLs on disease

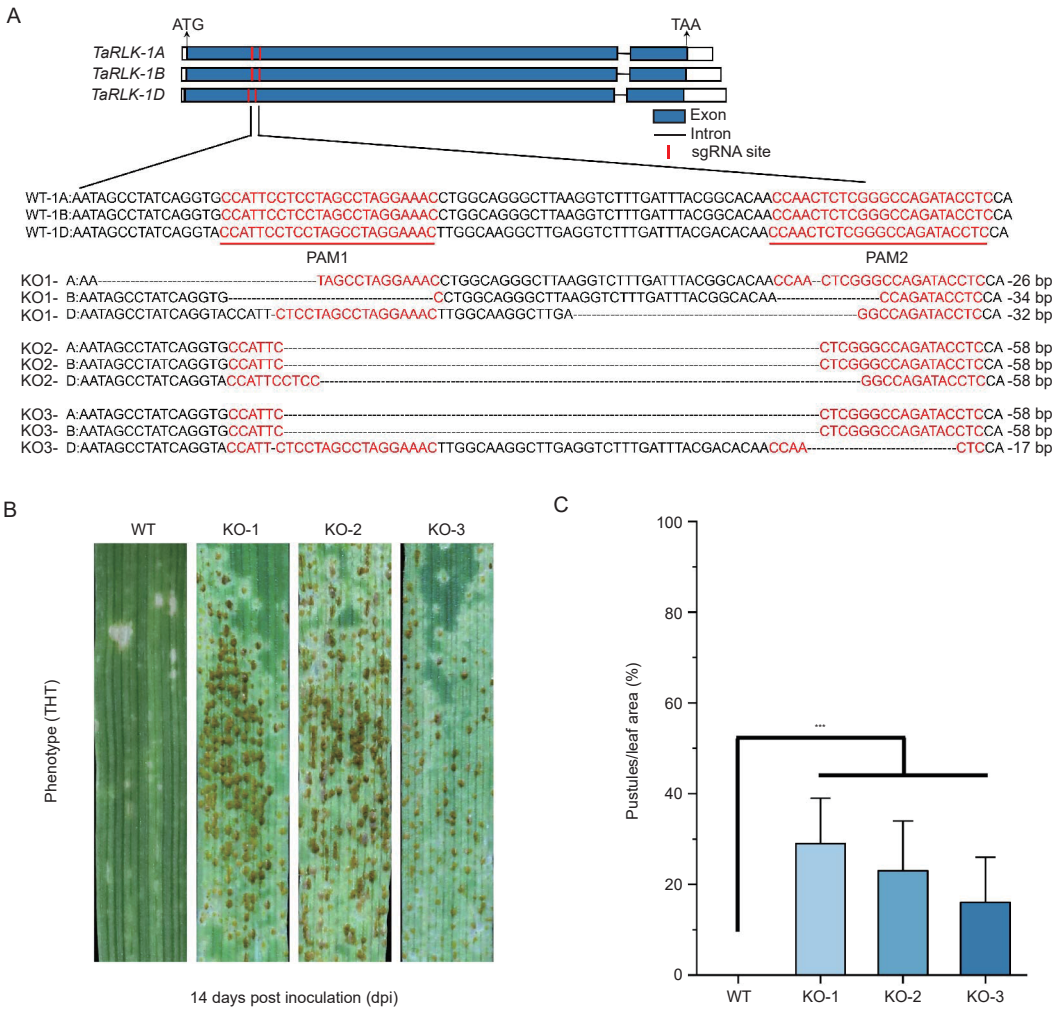

Fig. 5 Functional characterization of *TaRLK-1B via* a CRISPR-Cas9 gene editing strategy. A, strategy used to construct the knockout (KO) lines. The sequences of two sgRNA sites designed to target the conserved region of exon 1 among the three *TaRLK* homoeologs (top panel). Protospacer-adjacent motif (PAM) sequences are highlighted in red. The genotypes of the three mutants were recognized by sequencing, and the nucleotide mutations are shown in red (bottom panel). A dash (–) represents the deletion caused by CRISPR/Cas9-induced mutations. Numbers indicate the length of the deletion. B and C, disease symptoms and spore coverage quantification of wild type (WT) and KO seedling plants infected with *Pt* at 14 days post inoculation (dpi). Data are presented as the mean±SD (n=10). Significant differences were determined by Student's t-test (***, P<0.001).

resistance in the AB-NAMIC population was explored. An initial association analysis was performed using haplotypes defined by significant SNPs on chromosomes 1B, 2A, 2B, and 7D, and they were correlated with BLUP values. The findings revealed that germplasms with Hap-R presented significantly greater resistance to leaf rust than those with Hap-S. This finding indicates that the identified significant SNPs, which represent QTLs, can be used to effectively distinguish between resistant and susceptible haplotypes (Fig. 6-A; Appendix L). Building on these findings, the combined effects of four QTLs (*QLr.caas-1BL.2*, *QLr.caas-2AL*, *QLr.caas-2BS*, and *QLr.caas-7DL*) represented by significant SNPs, were found to form five unique haplotype combinations: HapC1 through HapC5. These combinations contain 0, 1, 2, 3, and 4 disease-resistant QTL alleles, respectively (Fig. 6-B and C). An association analysis with the BLUP values revealed a progressive improvement in plant resistance as the number of accumulated disease-resistance QTL alleles increased (Fig. 6-D). Therefore, pyramiding multiple QTLs significantly increases plant resistance, potentially offering substantial benefits for agricultural production by providing a more robust defense against this disease.

4. Discussion

4.1. Novel loci identified through GWAS provide valuable insights for the development of leaf rust resistant cultivars in wheat

In this study, a comprehensive field phenotypic assessment of 590 AB-NAMIC lines genotyped with a 660K SNP array was conducted and a GWAS analysis identified four QTLs: *QLr.caas-1BL.2*, *QLr.caas-2AL*, *QLr.caas-2BS*, and *QLr.caas-7DL*. Among them, *TaRLK-1B* was identified as a candidate gene for *QLr.caas-1BL.2*, and it was shown to play a positive regulatory role in wheat resistance to leaf rust (Fig. 5). On the long arm of chromosome 1B, the well-known multi-resistance gene *Lr46/Yr29/Sr58/Pm39/Ltn2* has been consistently identified as a major gene (Kolmer *et al.* 2015). This gene is located near our candidate interval. The Wheat55K SNP array was used to genotype a recombinant inbred line (RIL) population derived

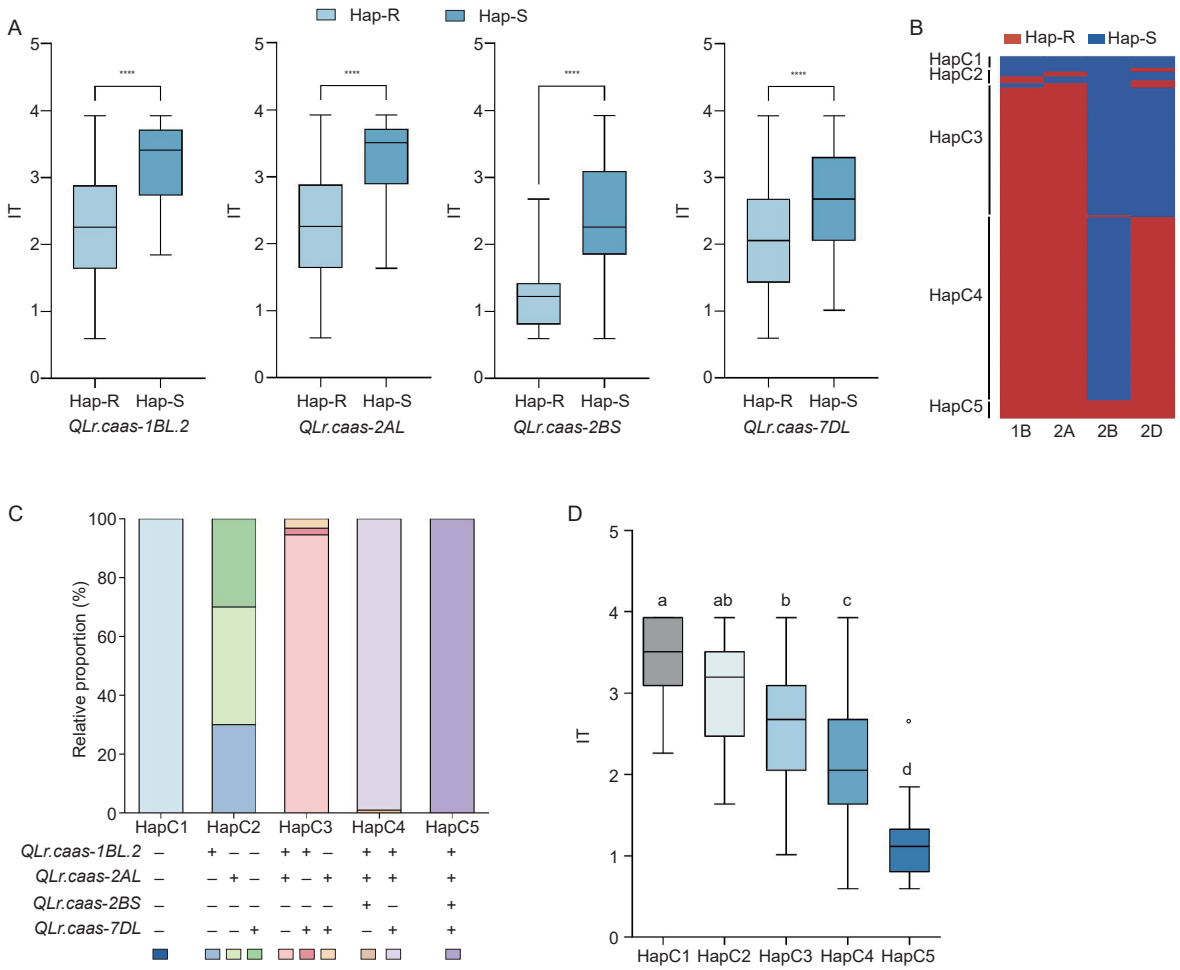

Fig. 6 Pyramiding of four QTLs for resistance to leaf rust. A, boxplot of the haplotype-phenotype association analysis results based on the best linear unbiased prediction (BLUP) values for four QTLs located on chromosomes 1B, 2A, 2B, and 7D. ****, $P<0.0001$ (two-tailed Student's *t*-test). B, heatmap depicting the different haplotype combinations associated with the four QTLs. C, overview of the QTL composition within each haplotype combination. D, boxplot of the haplotype combination-phenotype association analysis based on BLUP values. The middle line indicates the median, the box indicates the range of the 25th and 75th percentiles of the total data, the vertical lines indicate the interquartile range, and the outer circle represent outliers. IT, infection type. Different letters above the boxplots indicate significant differences according to Tukey's multiple comparisons test ($P<0.05$).

from Fuyu 3/Zhengzhou 5389, and the leaf rust resistance locus *QLr.hebau-1BL* and the stripe rust resistance locus *QYr.hebau-1BL* were localized to the 670.4–673.8 Mb region on chromosome 1BL, suggesting that these loci correspond to *Lr46/Yr29* (Gebrewahid *et al.* 2020). In addition, *QYr.ucw-1BL* may be the same locus as *Lr46/Yr29*, with a candidate interval identified between the flanking markers *ucw.k31* and *csLV46G22*, which spans a 332 kb region from 669.896 to 670.234 Mb and encompasses 10 candidate genes (Cobo *et al.* 2019). Recently, this interval has been further narrowed to 13.5 kb, with *TraesCS1B02G454200.1* being identified as a potential candidate gene (Spychała *et al.* 2024). Based on these findings, we speculate that *TaRLK-1B* and *Lr46/Yr29/Sr58/Pm39/Ltn2* are distinct genes, and that *TaRLK-1B* is a novel gene potentially responsible for conferring resistance to leaf rust.

Further analysis was conducted on the remaining three disease-resistance QTLs. *QLr.caas-2AL* was mapped to the interval between 759.7 and 769.6 Mb on chromosome 2AL. Four QTLs were also mapped on the long arm of chromosome 2A: *QLr.locus-2AL*, *QLr.ifa-2AL*, *QLr.hebau-2AL*, and *QLr.spa-2AL* (Ren *et al.* 2023). *QLr.locus-2AL* is positioned near the centromere (Aoun *et al.* 2016). According to marker information, the physical positions of the QTLs relative to the Chinese Spring reference sequence v1.0 are as follows: *QLr.ifa-2AL* at 709 Mb marked by *Xgwm312*; *QLr.hebau-2AL* at 728.6-729.3 Mb marked by *wmc181* and *BS00057060_51*; and *QLr.spa-2AL* at 701 Mb marked by *rPt-9611* (Buerstmayr *et al.* 2014; Singh *et al.* 2014; Zhang *et al.* 2017). These QTLs differ in position from *QLr.caas-2AL*, suggesting that *QLr.caas-2AL* may represent a novel locus. Furthermore, *QLr.caas-2BS* was mapped to the interval of 154.9–157.8 Mb on chromosome 2BS, a region known to harbor the major adult plant high-temperature resistance gene *Lr13*. Based on its location, we hypothesize that *QLr.caas-2BS* likely corresponds to the *Lr13* at 157.6 Mb (Yan *et al.* 2021). This QTL has demonstrated significant efficacy in mitigating leaf rust infection, suggesting that *Lr13* may indeed be responsible for the observed resistance (Fig. 6-A). On the long arm of chromosome 7D, only *Lr19*, located between 536.5 and 563.3 Mb marked by *Xgdm46* and *Xgdm67*, has been reported thus far (Prins *et al.* 2001; Gupta *et al.* 2006). In contrast, *QLr.caas-7DL* spans from 572.7 to 588.7 Mb, which is different from *Lr19*, indicating that *QLr.caas-7DL* may represent a novel resistance locus against leaf rust. The newly identified resistance QTLs provide valuable information for the breeding of wheat resistant to leaf rust.

4.2. Potential immune regulatory mechanisms of *TaRLK-1B*

Extensive research in model plants such as *Arabidopsis* and rice has highlighted the involvement of LRR-RLKs in the innate immune system (Ngou *et al.* 2022). A prominent example is the *Arabidopsis* LRR-RLK *FLS2*, which forms a heterodimer complex with its co-receptor BAK1 upon recognition of the bacterial flagellin peptide flg22, subsequently triggering the phosphorylation of RLCKs, which initiates a signaling cascade that includes the activation of MAPK cascades, generation of reactive oxygen species (ROS), influx of cytosolic calcium ions (Ca^{2+}), and activation of calcium-dependent protein kinases (CDPKs or CPKs) (Couto and Zipfel 2016; He *et al.* 2018). Despite their importance, the role of LRR-RLKs in the immune response of wheat to leaf rust remains largely unexplored. This study identified TaRLK-1B as a positive regulator of wheat resistance to the biotrophic fungus *Pt*, and it physically interacts with TaRLCK1B in tobacco (Fig. 5-B and C; Appendix K). Furthermore, Wu *et al.* (2020) reported that TaRLCK1B contributes to the immune response of wheat to *Rhizoctonia cerealis* by regulating the expression of enzymes involved in ROS generation and clearance, thereby maintaining ROS homeostasis (Wu *et al.* 2020). We hypothesize that after leaf rust infection, TaRLK-1B interacts with its coreceptor, leading to the phosphorylation of TaRLCK1B. This phosphorylation initiates a downstream signaling cascade that regulates ROS homeostasis, promotes protein and phenolic cross-linking, facilitates callose deposition, limits fungal invasion, and increases resistance to leaf rust. The intricate interplay among TaRLK-1B, its coreceptor, and TaRLCK1B underscores the need for further investigation to fully understand their roles in the defense mechanisms of wheat.

4.3. Pyramiding multiple QTLs for breeding resistant cultivars in wheat

In this study, the PVE values for the identified QTLs were relatively low, ranging from 0.46 to 9.57% (Appendix D). We speculate that this can be explained by the following two factors. First, the phenotypic assessment was performed on plants under natural field infections across limited years and locations, so they were subjected to marginal environmental conditions that contributed to environmental instability. Second, most of the detected QTLs are minor effect QTLs. Relatively low PVEs by adult plant resistance (APR) QTLs during the adult stage have also been reported in other studies (Zhang *et al.* 2021).

Although their individual contribution rates are relatively low, we found that the infection types of accessions carrying combinations of at least two resistance QTLs were significantly lower than those of accessions carrying only one of them, and that plant resistance gradually increased with the accumulation of resistance QTLs (Fig. 6-D). These findings underscore that pyramiding small- to intermediate-effect APR genes is important for effectively improving resistance to wheat leaf rust. Furthermore, compelling evidence indicates that combining multiple minor/intermediate effect APR genes can achieve high levels of resistance or near immunity (Lan *et al.* 2017; Yang *et al.* 2019; Ye *et al.* 2022). In future breeding practices, the pyramiding of multiple minor-effect QTLs resistant to various diseases should be considered to develop wheat varieties with durable resistance to multiple diseases. This approach aims to bolster the sustainability of resistance and increase the long-term effectiveness of crop disease management strategies.

5. Conclusion

In this study, a GWAS using the phenotypic data of adult plant resistance to leaf rust and genotypic data from 590 accessions of the AB-NAMIC population was used to identify

significant QTLs on chromosomes 1B, 2A, 2B, and 7D, with a particular emphasis on the candidate gene *TaRLK-1B* located on chromosome 1B. Based on the *TaRLK-1B* haplotypes, CAPS markers were developed that can distinguish resistant and susceptible haplotypes. This gene encodes a membrane-localized LRR-RLK that is upregulated during infection by the leaf rust fungus. Knocking out *TaRLK-1B* in wheat reduced resistance to leaf rust, indicating its positive regulatory role in disease defense. TaRLK-1B interacts with TaRLCK1B, potentially facilitating immune signal transduction. Furthermore, pyramiding minor-effect QTLs significantly increased resistance to leaf rust. This study contributes novel insights into resistance genes and valuable QTL information for leaf rust, which can aid in molecular marker-assisted breeding in wheat and expedite the development of new wheat varieties that are highly resistant to leaf rust disease.

Acknowledgements

This work was financially supported by the National Key Research and Development Program of China (2022YFF1003402), the National Natural Science Foundation of China (32272081 and 32161143007), and the Natural Science Foundation of Beijing, China (6242032).

Declaration of competing interest

The authors declare that they have no conflict of interest.

Declaration of generative AI and AI-assisted technologies in the writing process

The authors declare that they did not use AI in the preparation and writing of this manuscript.

Appendices associated with this paper are available at https://doi.org/10.1016/j.jia.2025.02.028

References

Aoun M, Breiland M, Turner M K, Loladze A, Chao S A M, Xu S S, Ammar K, Anderson J A, Kolmer J A, Acevedo M. 2016. Genome-wide association mapping of leaf rust response in a durum wheat worldwide germplasm collection. *The Plant Genome*, **9**, 1–24.

Buerstmayr M, Matiasch L, Mascher F, Vida G, Ittu M, Robert O, Holdgate S, Flath K, Neumayer A, Buerstmayr H. 2014. Mapping of quantitative adult plant field resistance to leaf rust and stripe rust in two European winter wheat populations reveals co-location of three QTL conferring resistance to both rust pathogens. *Theoretical and Applied Genetics*, **127**, 2011–2028.

Chen T T, Xiao J, Xu J, Wan W T, Qin B, Cao A Z, Chen W, Xing L P, Du C, Gao X Q, Zhang S Z, Zhang R Q, Shen W B, Wang H Y, Wang X E. 2016. Two members of TaRLK family confer powdery mildew resistance in common wheat. *BMC Plant Biology*, **16**, 27.

Cloutier S, McCallum B D, Loutre C, Banks T W, Wicker T, Feuillet C, Keller B, Jordan M C. 2007. Leaf rust resistance gene *Lr1*, isolated from bread wheat (*Triticum aestivum* L.) is a member of the large psr567 gene family. *Plant Molecular Biology*, **65**, 93–106.

Cobo N, Wanjugi H, Lagudah E, Dubcovsky J. 2019. A high-resolution map of wheat *QYr.ucw-1BL*, an adult plant stripe rust resistance locus in the same chromosomal region as *Yr29*. *The Plant Genome*, **12**, 1–15.

Couto D, Zipfel C. 2016. Regulation of pattern recognition receptor signalling in plants. *Nature Reviews Immunology*, **16**, 537–552.

Demirjian C, Vailleau F, Berthomé R, Roux F. 2023. Genome-wide association studies in plant pathosystems: Success or failure? *Trends in Plant Science*, **28**, 471–485.

Dracatos P M, Lu J, Sánchez-Martín J, Wulff B B H. 2023. Resistance that stacks up: Engineering rust and mildew disease control in the cereal crops wheat and barley. *Plant Biotechnology Journal*, **21**, 1938–1951.

Feuillet C, Travella S, Stein N, Albar L, Nublat A, Keller B. 2003. Map-based isolation of the leaf rust disease resistance gene *Lr10* from the hexaploid wheat (*Triticum aestivum* L.) genome. *Proceedings of the National Academy of Sciences of the United States of America*, **100**, 15253–15258.

Figueroa M, Hammond-Kosack K E, Solomon P S. 2018. A review of wheat diseases — A field perspective. *Molecular Plant Pathology*, **19**, 1523–1536.

Gebrewahid T W, Zhang P P, Zhou Y, Yan X C, Xia X C, He Z H, Liu D Q, Li Z F. 2020. QTL mapping of adult plant resistance to stripe rust and leaf rust in a Fuyu 3/Zhengzhou 5389 wheat population. *The Crop Journal*, **8**, 655–665.

Gupta S K, Charpe A, Prabhu K V, Haque Q M R. 2006. Identification and validation of molecular markers linked to the leaf rust resistance gene *Lr19* in wheat. *Theoretical and Applied Genetics*, **113**, 1027–1036.

Hao Y C, Kong F M, Wang L L, Zhao Y, Li M Y, Che N X, Li S, Wang M, Hao M, Zhang X C, Zhao Y. 2024. Genome-wide association study of grain micronutrient concentrations in bread wheat. *Journal of Integrative Agriculture*, **23**, 1468–1480.

He Y X, Zhou J G, Shan L B, Meng X Z. 2018. Plant cell surface receptor-mediated signaling — A common theme amid diversity. *Journal of Cell Science*, **131**, jcs209353.

Huai B Y, Yuan P, Ma X X, Zhang X R, Jiang L H, Zheng P J, Yao M H, Chen Z Y, Chen L Y, Shen Q H, Kang Z S, Liu J. 2022. Sugar transporter TaSTP3 activation by TaWRKY19/61/82 enhances stripe rust susceptibility in wheat. *New Phytologist*, **236**, 266–282.

Huang L, Brooks S A, Li W L, Fellers J P, Trick H N, Gill B S. 2003. Map-based cloning of leaf rust resistance gene *Lr21* from the large and polyploid genome of bread wheat. *Genetics*, **164**, 655–664.

Huerta-Espino J, Singh R P, Germán S, McCallum B D, Park R F, Chen W Q, Bhardwaj S C, Goyeau H. 2011. Global status of wheat leaf rust caused by *Puccinia triticina*. *Euphytica*, **179**, 143–160.

Ji X J, Xu S R, Wang Z Y, Han H M, Zhang J P, Zhou S H, Guo B J, Yang X M, Li X Q, Guo X M, Liu T G, Li L H, Liu W H. 2025. Identification of a genomic region controlling broad-spectrum immunity to leaf rust in wheat–*Agropyron cristatum* 2P translocation lines. *Journal of Integrative Agriculture*, **24**, 2015–2018.

Jian C, Hao P A, Hao C Y, Liu S J, Mao H D, Song Q L, Zhou Y B, Yin S N, Hou J, Zhang W J, Zhao H X, Zhang X Y, Li T. 2022. The miR319/TaGAMYB3 module regulates plant architecture and improves grain yield in common wheat (*Triticum aestivum*). *New Phytologist*, **235**, 1515–1530.

Jiao C Z, Hao C Y, Li T, Bohra A, Wang L F, Hou J, Liu H X, Liu H, Zhao J, Wang Y M, Liu Y C, Wang Z W, Jing X, Wang X E, Varshney R K, Fu J J, Zhang X Y. 2023. Fast integration and accumulation of beneficial breeding alleles through an AB-NAMIC strategy in wheat. *Plant Communications*, **4**, 100549.

Kang H M, Sul J H, Service S K, Zaitlen N A, Kong S Y, Freimer N B, Sabatti C, Eskin E. 2010. Variance component model to account for sample structure in genome-wide association studies. *Nature Genetics*, **42**, 348–354.

Kaur S, Gill H S, Breiland M, Kolmer J A, Gupta R, Sehgal S K, Gill U. 2023. Identification of leaf rust resistance loci in a geographically diverse panel of wheat using genome-wide association analysis. *Frontiers in Plant Science*, **14**, 1090163.

Kolmer J. 2013. Leaf rust of wheat: Pathogen biology, variation and host resistance. *Forests*, **4**, 70–84.

Kolmer J A, Lagudah E S, Lillemo M, Lin M, Bai G. 2015. The *Lr46* gene conditions partial adult-plant resistance to stripe rust, stem rust, and powdery mildew in thatcher wheat. *Crop Science*, **55**, 2557–2565.

Kolodziej M C, Singla J, Sánchez-Martín J, Zbinden H, Šimková H, Karafiátová M, Doležel J, Gronnier J, Poretti M, Glauser G, Zhu W S, Köster P, Zipfel C, Wicker T, Krattinger S G, Keller B. 2021. A membrane-bound ankyrin repeat protein confers race-specific leaf rust disease resistance in wheat. *Nature Communications*, **12**, 956.

Krattinger S G, Lagudah E S, Spielmeyer W, Singh R P, Huerta-Espino J, McFadden H, Bossolini E, Selter L L, Keller B. 2009. A putative ABC transporter confers durable resistance to multiple fungal pathogens in wheat. *Science*, **323**, 1360–1363.

Lan C X, Basnet B R, Singh R P, Huerta-Espino J, Herrera-Foessel S A, Ren Y, Randhawa M S. 2017. Genetic analysis and mapping of

adult plant resistance loci to leaf rust in durum wheat cultivar Bairds. *Theoretical and Applied Genetics*, **130**, 609–619.
Li H N, Hua L, Zhao S Q, Hao M, Song R, Pang S Y, Liu Y N, Chen H, Zhang W J, Shen T, Gou J Y, Mao H L, Wang G P, Hao X H, Li J, Song B X, Lan C X, Li Z F, Deng X W, Dubcovsky J, *et al.* 2023. Cloning of the wheat leaf rust resistance gene *Lr47* introgressed from *Aegilops speltoides*. *Nature Communications*, **14**, 6072.
Li J H, Zhang S J, Zhang R Z, Gao J, Qi Y P, Song G Q, Li W, Li Y L, Li G Y. 2021. Efficient multiplex genome editing by CRISPR/Cas9 in common wheat. *Plant Biotechnology Journal*, **19**, 427–429.
Lin G F, Chen H, Tian B, Sehgal S K, Singh L, Xie J Z, Rawat N, Juliana P, Singh N, Shrestha S, Wilson D L, Shult H, Lee H, Schoen A W, Tiwari V K, Singh R P, Guttieri M J, Trick H N, Poland J, Bowden R L, *et al.* 2022. Cloning of the broadly effective wheat leaf rust resistance gene *Lr42* transferred from *Aegilops tauschii*. *Nature Communications*, **13**, 3044.
Liu S J, Liu H, Guo M J, Pan Y X, Hao C Y, Hou J, Yan L L, Zhang X Y, Chen X H, Li T. 2024. Knockout of GRAIN WIDTH2 has a dual effect on enhancing leaf rust resistance and increasing grain weight in wheat. *Plant Biotechnology Journal*, **22**, 2007–2009.
Liu Y C, Xi W, Wang X L, Li H F, Liu H X, Li T, Hou J, Liu X, Hao C Y, Zhang X Y. 2023. TabHLH95-TaNF-YB1 module promotes grain starch synthesis in bread wheat. *Journal of Genetics and Genomics*, **50**, 883–894.
Moore J W, Herrera-Foessel S, Lan C X, Schnippenkoetter W, Ayliffe M, Huerta-Espino J, Lillemo M, Viccars L, Milne R, Periyannan S, Kong X Y, Spielmeyer W, Talbot M, Bariana H, Patrick J W, Dodds P, Singh R, Lagudah E. 2015. A recently evolved hexose transporter variant confers resistance to multiple pathogens in wheat. *Nature Genetics*, **47**, 1494–1498.
Ngou B P M, Ding P T, Jones J D G. 2022. Thirty years of resistance: Zig-zag through the plant immune system. *The Plant Cell*, **34**, 1447–1478.
Pang Y L, Wu Y Y, Liu C X, Li W H, St Amand P, Bernardo A, Wang D F, Dong L, Yuan X F, Zhang H R, Zhao M, Li L Z, Wang L M, He F, Liang Y L, Yan Q, Lu Y, Su Y, Jiang H M, Wu J J, *et al.* 2021. High-resolution genome-wide association study and genomic prediction for disease resistance and cold tolerance in wheat. *Theoretical and Applied Genetics*, **134**, 2857–2873.
Prasad P, Savadi S, Bhardwaj S C, Gupta P K. 2020. The progress of leaf rust research in wheat. *Fungal Biology*, **124**, 537–550.
Prins R, Groenewald J Z, Marais G F, Snape J W, Koebner R M D. 2001. AFLP and STS tagging of *Lr19*, a gene conferring resistance to leaf rust in wheat. *Theoretical and Applied Genetics*, **103**, 618–624.
Ren X P, Wang C Y, Ren Z, Wang J, Zhang P P, Zhao S Q, Li M Y, Yuan M, Yu X M, Li Z F, Chen S S, Wang X D. 2023. Genetics of resistance to leaf rust in wheat: An overview in a genome-wide level. *Sustainability*, **15**, 3247.
Savary S, Willocquet L, Pethybridge S J, Esker P, McRoberts N, Nelson A. 2019. The global burden of pathogens and pests on major food crops. *Nature Ecology & Evolution*, **3**, 430–439.
Sharma D, Avni R, Gutierrez-Gonzalez J, Kumar R, Sela H, Prusty M R, Shatil-Cohen A, Molnár I, Holušová K, Said M, Doležel J, Millet E, Khazan-Kost S, Landau U, Bethke G, Sharon O, Ezrati S, Ronen M, Maatuk O, Eilam T, *et al.* 2024. A single NLR gene confers resistance to leaf and stripe rust in wheat. *Nature Communications*, **15**, 9925.
Shin J H, Blay S, Graham J, McNeney B. 2006. LDheatmap: An R function for graphical display of pairwise linkage disequilibria between single nucleotide polymorphisms. *Journal of Statistical Software*, **16**, 1–9.
Shiu S H, Bleecker A B. 2001. Receptor-like kinases from *Arabidopsis* form a monophyletic gene family related to animal receptor kinases. *Proceedings of the National Academy of Sciences of the United States of America*, **98**, 10763–10768.
Singh A, Knox R E, DePauw R M, Singh A K, Cuthbert R D, Campbell H L, Shorter S, Bhavani S. 2014. Stripe rust and leaf rust resistance QTL mapping, epistatic interactions, and co-localization with stem rust resistance loci in spring wheat evaluated over three continents. *Theoretical and Applied Genetics*, **127**, 2465–2477.
Smakowska-Luzan E, Mott G A, Parys K, Stegmann M, Howton T C, Layeghifard M, Neuhold J, Lehner A, Kong J X, Grünwald K, Weinberger N, Satbhai S B, Mayer D, Busch W, Madalinski M, Stolt-Bergner P, Provart N J, Mukhtar M S, Zipfel C, Desveaux D, *et al.* 2018. An extracellular network of *Arabidopsis* leucine-rich repeat receptor kinases. *Nature*, **553**, 342–346.
Spychała J, Tomkowiak A, Noweiska A, Bobrowska R, Bocianowski J, Sobiech A, Kwiatek M T. 2024. Diversity of expression patterns of *Lr34*, *Lr67*, and candidate genes towards *Lr46* with analysis of associated miRNAs in common wheat hybrids in response to *Puccinia triticina* fungus. *Current Issues in Molecular Biology*, **46**, 5511–5529.
Thind A K, Wicker T, Šimková H, Fossati D, Moullet O, Brabant C, Vrána J, Doležel J, Krattinger S G. 2017. Rapid cloning of genes in hexaploid wheat using cultivar-specific long-range chromosome assembly. *Nature Biotechnology*, **35**, 793–796.
Tong J Y, Zhao C, Liu D, Jambuthenne D T, Sun M J, Dinglasan E, Periyannan S K, Hickey L T, Hayes B J. 2024. Genome-wide atlas of rust resistance loci in wheat. *Theoretical and Applied Genetics*, **137**, 179.
Wang J H, Wang J J, Shang H S, Chen X M, Xu X M, Hu X P. 2019. *TaXa21*, a leucine-rich repeat receptor-like kinase gene associated with *TaWRKY76* and *TaWRKY62*, plays positive roles in wheat high-temperature seedling plant resistance to *Puccinia striiformis* f. sp. *tritici*. *Molecular Plant-Microbe Interactions*, **32**, 1526–1535.
Wang Y J, Abrouk M, Gourdoupis S, Koo D H, Karafiátová M, Molnár I, Holušová K, Doležel J, Athiyannan N, Cavalet-Giorsa E, Jaremko Ł, Poland J, Krattinger S G. 2023. An unusual tandem kinase fusion protein confers leaf rust resistance in wheat. *Nature Genetics*, **55**, 914–920.
Wu T C, Zhu X L, Lv L J, Chen X Y, Xu G B, Zhang Z Y. 2020. The wheat receptor-like cytoplasmic kinase TaRLCK1B is required for host immune response to the necrotrophic pathogen *Rhizoctonia cerealis*. *Journal of Integrative Agriculture*, **19**, 2616–2627.
Xu S R, Ji X J, Han H M, Zhang J P, Zhou S H, Guo B J, Yang X M, Li X Q, Guo X M, Liu T G, Li L H, Liu W H. 2024. *AcRLK2P-1*, an LRR receptor protein kinase gene from *Agropyron cristatum*, confers leaf rust resistance in wheat. *Plant Communications*, **5**, 101132.
Yan X C, Li M M, Zhang P P, Yin G H, Zhang H Z, Gebrewahid T W, Zhang J P, Dong L L, Liu D Q, Liu Z Y, Li Z F. 2021. High-temperature wheat leaf rust resistance gene *Lr13* exhibits pleiotropic effects on hybrid necrosis. *Molecular Plant*, **14**, 1029–1032.
Yang J, Lee S H, Goddard M E, Visscher P M. 2011. GCTA: A tool for genome-wide complex trait analysis. *The American Journal of Human Genetics*, **88**, 76–82.
Yang M Y, Li G R, Wan H S, Li L P, Li J, Yang W Y, Pu Z J, Yang Z J, Yang E N. 2019. Identification of QTLs for stripe rust resistance in a recombinant inbred line population. *International Journal of Molecular Sciences*, **20**, 3410.
Yao L S, Li Y M, Ma C Y, Tong L X, Du F L, Xu M L. 2020. Combined genome-wide association study and transcriptome analysis reveal candidate genes for resistance to *Fusarium* ear rot in maize. *Journal of Integrative Plant Biology*, **62**, 1535–1551.
Ye B W, Singh R P, Yuan C, Liu D M, Randhawa M S, Huerta-Espino J, Bhavani S, Lagudah E, Lan C X. 2022. Three co-located resistance genes confer resistance to leaf rust and stripe rust in wheat variety Borlaug 100. *The Crop Journal*, **10**, 490–497.
Zhang P P, Yan X C, Gebrewahid T W, Zhou Y, Yang E N, Xia X C, He Z H, Li Z F, Liu D Q. 2021. Genome-wide association mapping of leaf rust and stripe rust resistance in wheat accessions using the 90K SNP array. *Theoretical and Applied Genetics*, **134**, 1233–1251.
Zhang P P, Yin G H, Zhou Y, Qi A Y, Gao F M, Xia X C, He Z H, Li Z F, Liu D Q. 2017. QTL mapping of adult-plant resistance to leaf rust in the wheat cross Zhou 8425B/Chinese Spring using high-density SNP markers. *Frontiers in Plant Science*, **8**, 793.
Zhang Z W, Ersoz E, Lai C Q, Todhunter R J, Tiwari H K, Gore M A, Bradbury P J, Yu J M, Arnett D K, Ordovas J M, Buckler E S. 2010. Mixed linear model approach adapted for genome-wide association studies. *Nature Genetics*, **42**, 355–360.

Managing Editor Ning Wang